

Deep Compositional Models for Non-Stationary Extremal Dependence

Xuanjie Shao Jordan Richards* Raphaël Huser

Statistics Program, CEMSE Division, KAUST

جامعة الملك عبد الله
للعلوم والتقنية
King Abdullah University of
Science and Technology



Introduction

- Modeling **non-stationarity** in **extremal dependence** is challenging, while inference for stationary and isotropic models is considerably easier.
- Deformation approach** (Sampson and Guttorp, 1992): warp the original domain \mathcal{G} to a latent space \mathcal{W} where stationarity/isotropy can be reasonably assumed.
- Consider a spatial process $Z(\cdot)$ on \mathcal{G} with finite variance for each $\mathbf{s} \in \mathcal{S}_0 \subset \mathcal{G}$. Estimation of the warping function $\mathbf{f} : \mathcal{G} \rightarrow \mathcal{W}$ is problematic: computationally expensive, lacking in flexibility, and not injective.
- Deep composition modeling approach** (Zammit-Mangion et al., 2022): transformation is constructed using a series of n injective warping functions,

$$\mathbf{f}(\cdot) \equiv \mathbf{f}_n \circ \mathbf{f}_{n-1} \circ \dots \circ \mathbf{f}_1(\cdot).$$
- We present an extension of this methodology to spatial extremal processes, using the R interface to **TensorFlow 2**.

Deep Compositional Model (DCM)

The DCM comprises n layers in a neural network, with

$$\mathbf{f}_i(\mathbf{s}) = \mathbf{W}_i \phi_i(\mathbf{s}; \Theta_i) : D_{i-1} \rightarrow D_i, \quad i = 1, \dots, n,$$

mapping the input to a d_i -dimensional output for $D_i \subset \mathbb{R}^{d_i}$, $D_0 \equiv \mathcal{G}$, and $D_n \equiv \mathcal{W}$.

- $\phi_i(\cdot; \Theta_i)$: basis functions at the i -th layer with parameters Θ_i .
- \mathbf{W}_i : weights for the basis-functions at the i -th layer.

Different choices for ϕ_i lead to different types of warping units.

- Axial Warping Unit (AWU)**: \mathbf{f}_i models nonlinear scaling of one input dimension.
- Radial Basis Function (RBF)**: \mathbf{f}_i describes local expansions/contractions at various resolutions.
- Möbius Transformation**: \mathbf{f}_i performs a rotation in the complex plane.

Brown–Resnick Process

Brown–Resnick (BR) Process

- The Brown–Resnick process is a max-stable process that can be expressed as

$$Z(\mathbf{s}) = \sup_{i \geq 1} U_i(\mathbf{s})/P_i,$$

where P_i 's are Poisson point processes on \mathbb{R}_+ with unit rate intensity, and $U_i(\mathbf{s})$ are i.i.d. copies of a non-negative stochastic process

$$U(\mathbf{s}) = \exp\{\epsilon(\mathbf{s}) - \sigma^2(\mathbf{s})/2\}, \quad \mathbf{s} \in \mathcal{S},$$

for an intrinsically-stationary Gaussian process $\epsilon(\mathbf{s})$ with variance $\sigma^2(\mathbf{s})$, $\epsilon(\mathbf{0}) \stackrel{a.s.}{=} 0$, and semivariogram $\gamma(h) = (h/\varphi)^\kappa$ with range $\varphi > 0$ and smoothness $\kappa \in (0, 2]$.

- The bivariate joint distribution function of Z is $\Pr\{Z(\mathbf{s}_1) \leq z_1, Z(\mathbf{s}_2) \leq z_2\} = \exp\{-V(z_1, z_2)\}$, where V is the **bivariate exponent function**

$$V(z_1, z_2) = z_1^{-1} \Phi\{a/2 - a^{-1} \log(z_1/z_2)\} + z_2^{-1} \Phi\{a/2 - a^{-1} \log(z_2/z_1)\},$$

with $a = \{2\gamma(h)\}^{1/2}$ and $h = \|\mathbf{s}_1 - \mathbf{s}_2\|$.

- Extremal coefficient (EC)** measures extremal dependence between sites $\mathbf{s}_1, \mathbf{s}_2$, denoted $\theta(\mathbf{s}_1, \mathbf{s}_2) = V(1, 1) = 2\Phi\{\sqrt{2\gamma(h)}/2\} \in [1, 2]$.

Inference

- Pairwise likelihood (PL)**: ℓ_{PL} with dependence parameters $\boldsymbol{\psi}$ is

$$\ell_{PL}(\boldsymbol{\psi}) = \sum_{t=1}^T \sum_{\mathbf{s}_1, \mathbf{s}_2 \in \mathcal{S}} \ell_{PL}(z_{t,1}, z_{t,2}; \boldsymbol{\psi})$$

where $z_{t,i}$ is t -th block maxima at $\mathbf{s}_i \in \mathcal{W}$, and ℓ_{PL} represents the corresponding pairwise log-density.

To save time \Rightarrow Careful choice of a suitable smaller number of pairs.

- Least squares inference through extremal coefficients**: using empirical bivariate extremal coefficients $\hat{\theta}_2(\mathbf{s}_1, \mathbf{s}_2)$,

$$\ell_{EC}(\boldsymbol{\psi}) = \sum_{\mathbf{s}_1, \mathbf{s}_2 \in \mathcal{S}} \left\{ \hat{\theta}_2(\mathbf{s}_1, \mathbf{s}_2) - \theta_2(\mathbf{s}_1, \mathbf{s}_2; \boldsymbol{\psi}) \right\}^2.$$

- The joint loss function**: with the original spatial locations $\mathcal{S}_0 \subset \mathcal{G}$,

$$L(\boldsymbol{\psi}, \Theta, \mathbf{W}; \mathcal{S}_0) = \ell(\boldsymbol{\psi}; \mathcal{S}_n),$$

where the warped locations $\mathcal{S}_n = \mathbf{f}(\mathcal{S}_0; \Theta, \mathbf{W}) \subset \mathcal{W}$. Here $\mathbf{W} = \{\mathbf{W}_1, \dots, \mathbf{W}_n\}$, $\Theta = \{\Theta_1, \dots, \Theta_n\}$ are weights and parameters in the DCM.

We can take $\ell(\boldsymbol{\psi}; \mathcal{S}_n)$ to be either $-\ell_{PL}(\boldsymbol{\psi})$ or $\ell_{EC}(\boldsymbol{\psi})$.

References

- Sampson, P. D. and Guttorp, P. (1992). Nonparametric estimation of nonstationary spatial covariance structure. *Journal of the American Statistical Association*, 87(417):108–119.
- Shao, X., Hazra, A., Richards, J., and Huser, R. (2022). Flexible modeling of nonstationary extremal dependence using spatially-fused LASSO and ridge penalties. *arXiv preprint arXiv:2210.05792*.
- Zammit-Mangion, A., Ng, T. L. J., Vu, Q., and Filippone, M. (2022). Deep compositional spatial models. *Journal of the American Statistical Association*, 117(540):1787–1808.

Simulation Study

- Simulated data over a warped domain (generated with 2 AWUs and an RBF unit) on a 101×101 grid are generated from a **stationary BR process** with $\varphi = 0.1$ and $\kappa = 1$. $D = 2000$ locations are chosen randomly for inference, with 100 independent replications held out for training.
- The deep compositional model consists of AWUs for each input axis, one RBF, and a Möbius transformation. Both PL and EC inference methods are used to reconstruct the warped space.
- Computation time for PCL inference using **1% (100%) pairs** is **1h (7h)**; computation time for EC inference is generally **less than 1h**.

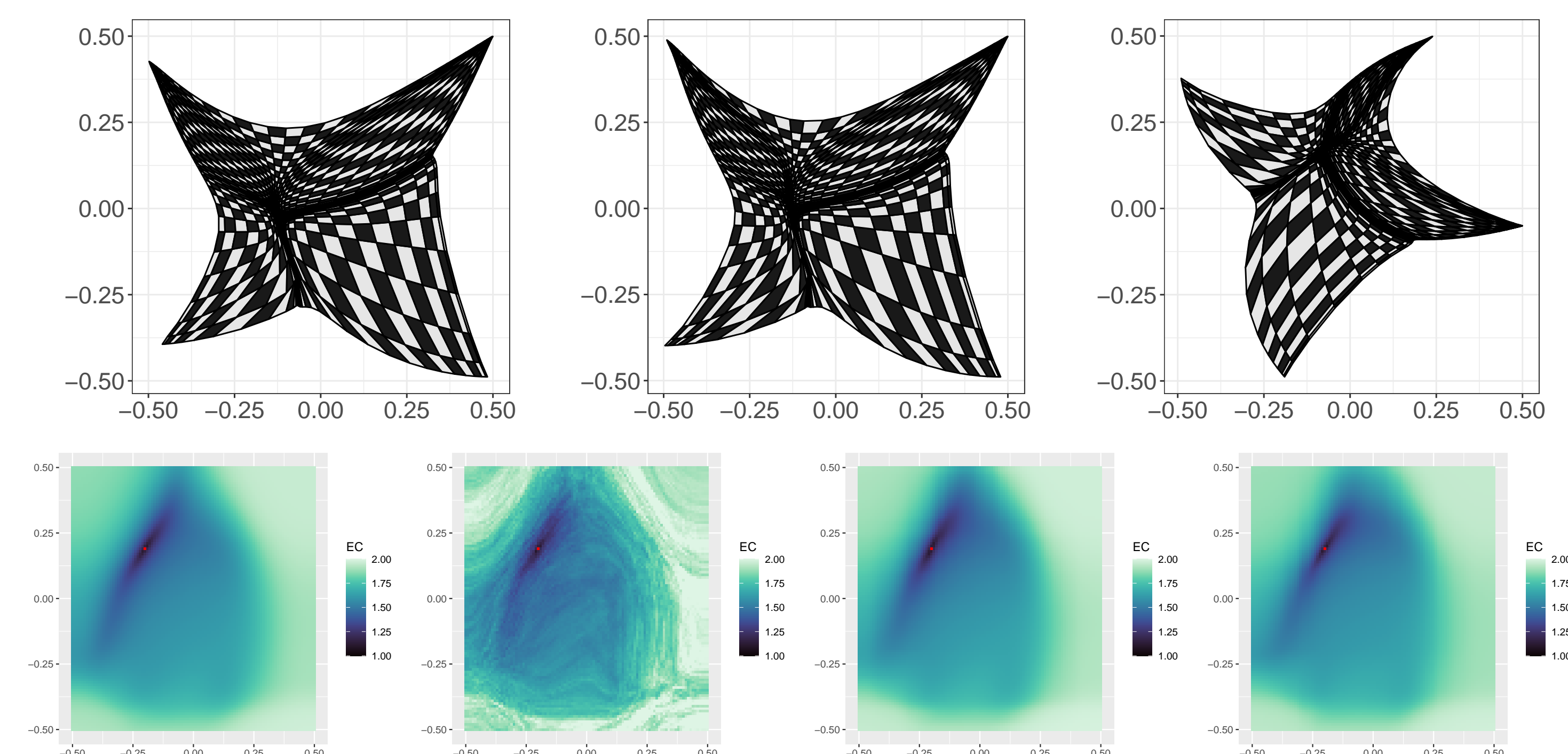


Figure 1. Top: true (left), and fitted (PCL: middle; EC: right) space; Bottom: theoretical and empirical pairwise ECs (1st, 2nd), fitted pairwise ECs (PCL: 3rd; EC: 4th) relative to the reference site in red.

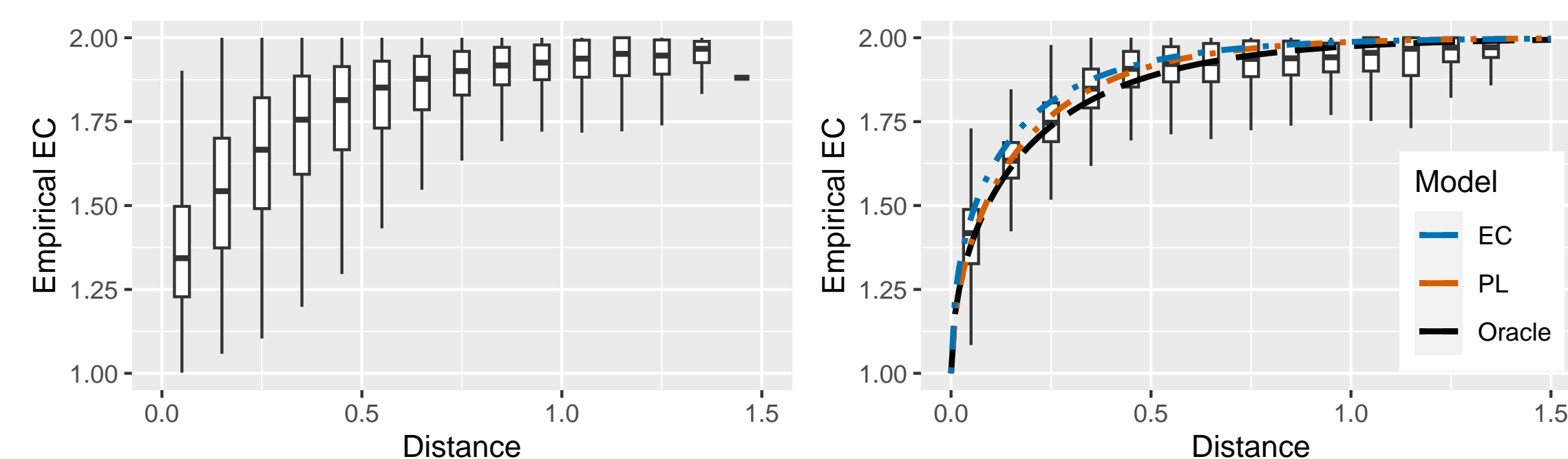


Figure 2. Boxplot of empirical ECs against distance (left: original space; right: warped space), and model EC curves.

Application: Monthly Temperature Maxima over Nepal

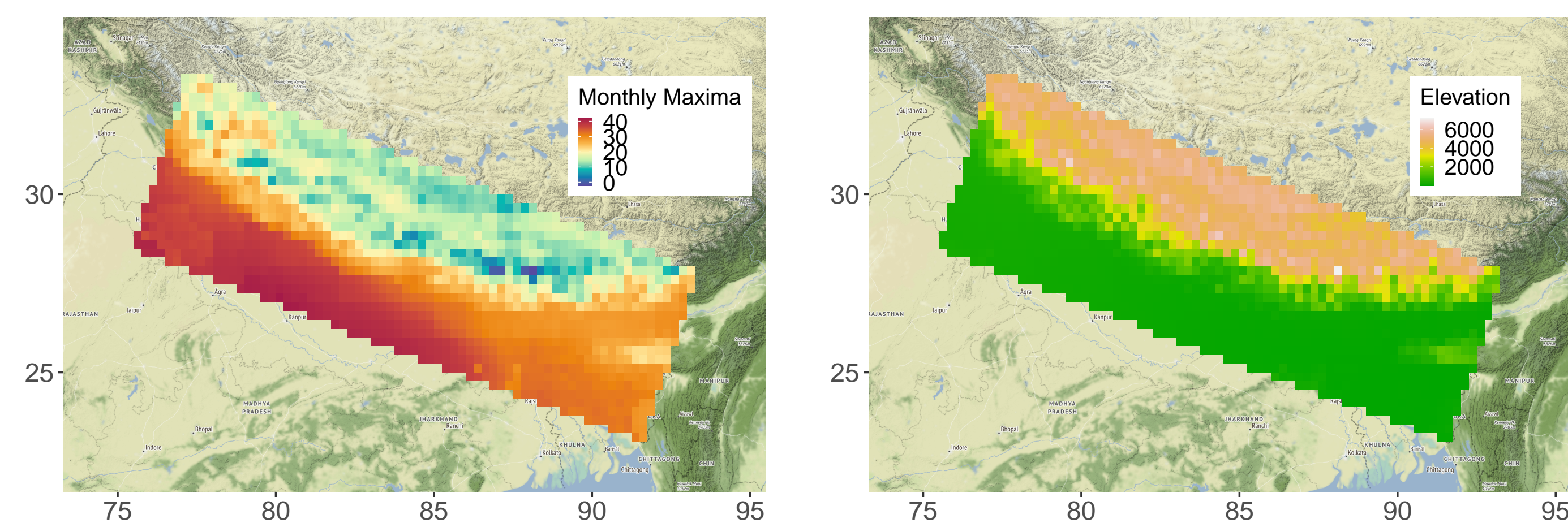


Figure 3. Left: one observed monthly maxima ($^{\circ}\text{C}$); right: elevation of the spatial domain.

- Monthly maxima** of daily average temperatures with $D = 1417$ sites and $T = 192$ replications, with **unit Fréchet margins**.
- Previously analysed by Shao et al. (2022) with a locally-stationary model.
- Elevation information is further introduced, which improve the modeling of some spatial areas, e.g., around Everest.

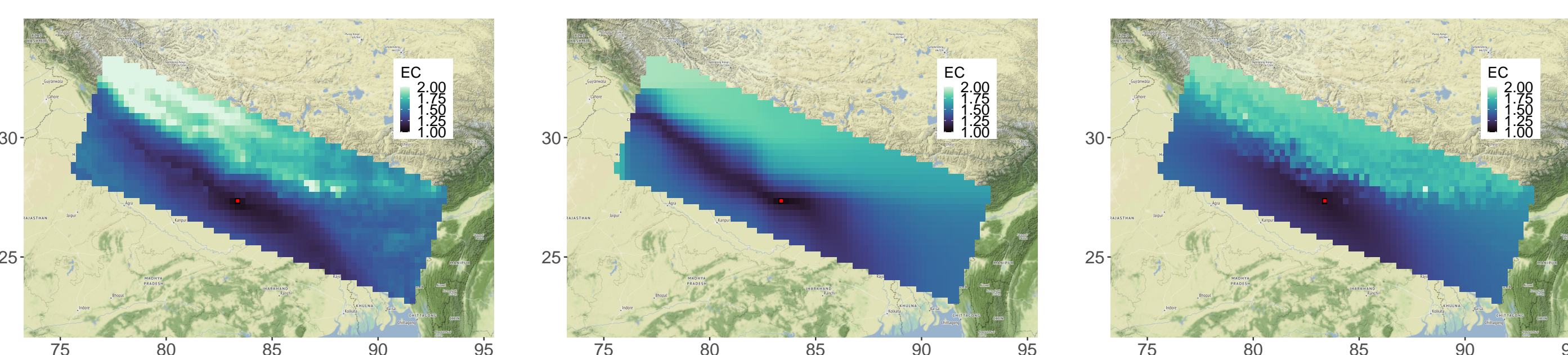


Figure 4. Left: empirical pairwise ECs; middle: fitted pairwise ECs (relative to a reference site; red) based on the DCM with a Brown–Resnick process (using least squares inference); right: fitted pairwise ECs incorporating elevation in \mathcal{G} .

Future Work

- Extension to **other extremal processes**, e.g., r -Pareto processes, inverted BR.
- Modeling temporal changes, uncertainty assessment, new warping units.